CUBESAT CLUSTER DEPLOYMENT TRACKING WITH A CPHD FILTER

John A. Gaebler[*] and Penina Axelrad[†]

Clustered CubeSat deployments, where multiple CubeSats are released over a short time span, represent a relatively new and challenging detection and tracking problem. The last two decades have seen a growing interest in multi-target, multi-sensor filtering methods with the filters applied to simulations highlighting advancements. This work applies the Cardinalized Probability Hypothesis Density filter to a realistic tracking scenario, a clustered CubeSat deployment modeled after the recent launch of 104 satellites from the Indian PSLV-C37. The filter is assessed to gauge the effectiveness under non-ideal circumstances including weak observation geometry, realistic measurement noise, sparse data with large time gaps between contacts, and nonlinear dynamics. Tuning of the filter is discussed in the context of a cluster deployment. Methods of assessing the results are presented and discussed. Results show that the CPHD filter is capable of estimating the location of targets in a cluster launch, but not without several complications which bring into question the applicability of the filter to a cluster deployment.

INTRODUCTION

To date there have been over 600 CubeSats successfully launched into orbit[‡]. The most recent deployment being an Indian PSLV-C37 mission that released 104 satellites (which included 88 Planet Labs 3U CubeSats) into space on February 15 2017. This clear industry trend toward increasingly large deployments of small satellites poses a new challenge for space object tracking and space traffic management. The goal of this work is to investigate multi-target tracking algorithms and the sensor configurations that will provide timely and accurate tracking solutions of a clustered deployment scenario without direct communication with the satellites.

Over the last few years CubeSat missions have reported on the difficulty of relying on Two Line Elements (TLEs) provided by the Joint Space Operations Center (JSpOC) early in the mission[1,2]. Researchers and industry professionals have begun advocating policy changes to push CubeSat developers toward adding navigation aids, in the form of ID beacons or reflectors, to make CubeSats easier to track [3,4]. On the forefront is Radio Frequency Identification (RFID) whereby each satellite emits a unique beacon[4]. Beacons will aid in the correlation of observations to the correct satellites. To make CubeSats easier to track there are recommendations to install corner reflectors or reflective tape, both for radar and optical wavelengths[5]. Beyond hardware changes and additions to the CubeSats, there are also policy recommendations to control mission parameters, such as

[*] PhD Student, Smead Aerospace Engineering Sciences, University of Colorado, 431 UCB, Boulder, Colorado 80309.
[†] Professor, Smead Aerospace Engineering Sciences, University of Colorado, 431 UCB, Boulder, Colorado 80309.
[‡] Kulu, E. (n.d.). Nanosatellite Database by Erik. Retrieved Oct 11, 2016, from http://www.nanosats.eu/

restricting CubeSats to orbital altitudes less than 500 km, or requiring maneuverability if operating in high risk regions[6].

A policy that has helped reduce the time to perform initial tracking of CubeSats has been the sharing of tracking and identification data. JSpOC has a sharing program to ingest operator data to aid in proper identification of satellites[1,3]. The most useful data that can be shared with JSpOC comes from GPS derived solutions of the CubeSat positions. GPS can provide very accurate position estimates, but to downlink their GPS solutions, the CubeSats must still be contacted for the first time using tracking data provided by other means.

From the point of view of government sponsored Space Situational Awareness (SSA) activities, the focus is on tracking all space objects, irrespective of cooperation or compliance by satellite operators. It is toward this end that the current work evaluates the capabilities of multi-target multi-sensor estimation algorithms relying on ground based observations without the benefit of onboard navigation aids, tracking tags or satellite operator provided data.

Robust tracking in cluttered scenarios will depend on tracking algorithms that can handle multiple targets and observation types simultaneously. New methods are being developed around probabilistic association and hypothesis testing. Reference 7 discusses the importance of multi-object filtering techniques in SSA. Multi-target methods based on random finite sets are crucial because of the difficulty in observing individual CubeSats when there are many in close proximity. Probability Hypothesis Density (PHD) filters utilize the probabilistic likelihood of objects being present at particular locations in the state space. This work studies the Cardinalized PHD (CPHD) filter. The CPHD has the benefit of estimating the cardinality, or number of targets present. There is a major disadvantage however. The CPHD is strictly speaking, an estimator. It does not track specific targets (labels). There are more advanced filters in the literature which include labels and therefor can be correctly called trackers, such as the Generalized Labeled Multi-Bernoulli (GLMB) filter[8].

This work starts with the CPHD, since from the point of view of the SSA establishment, the need is to know where objects are located. The effectiveness of the CPHD filter on a realistic and complex early mission tracking problem assuming uncooperative satellites is investigated. This work serves as a precursor to future efforts to develop robust tracking and detection strategies for the deployment of multiple CubeSats. Future work will test the capabilities developed here against labeled multi-target filters.

CLUSTERED DEPLOYMENT SCENARIO

The February 2017 launch of 104 satellites serves as the basis for this study. Although the full launch included a variety of satellite types, we focus on the 88 Planet Labs Flock III Cubesats that were deployed. The simulation includes 89 unique objects, the "Doves" plus the deployment vehicle. Lacking access to detailed operational data for this commercial launch, aspects of the deployment strategy were inferred from articles and videos posted of the launch[*]. From the publicly available information, we constructed a representative simulation. The simulated deployment strategy is composed of two simultaneous launches every 2 seconds in opposite directions (starting in the + and – local velocity direction of the launch vehicle) with a 10 second gap after every 10^{th} pair until all 88 Doves are deployed. Thus, half of the Cubesats are deployed in the forward direction relative to the deployer velocity, while the other half are launched in the backward direction, causing there to be two distinct clusters of Cubesats slowly separating due to natural orbital dynamics.

[*] Department of Space Indian Space Research Organisation. Retrieved March 6, 2017. http://www.isro.gov.in/pslv-c37-cartosat-2-series-satellite/pslv-c37-lift-and-onboard-camera-video

The Keplerian elements of the deployment vehicle are given in Table 1. Deployment is assumed to use compressed springs to impart the needed delta-velocity (DV). Assuming the deployment system was similar to a Poly-Picosatellite Orbital Deployer (P-POD), a nominal value of 1.5 m/s DV was used for all deployments[9]. The actual deployment vehicle's spinning motion about the angular momentum vector adds complexity to the scenario. This is modeled as a slow rotation from the initial orientation in the along-track direction, towards a final orientation in the radial direction at the end of the deployment phase. Hence the Cubesats have velocities imparted in both the in-track and radial directions relative to the deployer.

Table 1: Keplerian orbital elements of deployment vehicle

Semi-major axis	Eccentricity	Inclination	Right-ascension of ascending node	Argument of peri-gee
6869.9 km	**0.00132**	**97.6°**	**108.1°**	**216°**

Uncertainties are added at several stages of the deployment during a filter run. The initial condition of the deployer is randomly perturbed using a prescribed Radial, In-track, Cross-track (RIC) covariance with a sigma of 5 meters in positions and 0.5 mm/s in velocities. A rotation rate error of 1% is applied. Finally, variations in the DV are applied as random 1% errors in the magnitude of the velocity relative to the rocket body. To test and tune the filter, the motion of all Cubesats after deployment is assumed to be purely Keplerian.

SIMULATION OBSERVABLES

Focusing on the SSA aspect of tracking an uncooperative deployment, U.S. radar tracking stations are simulated. Three stations were chosen to include in the simulation located at: Eglin AFB in Florida, Shemya Alaska, and Cavalier AFB in North Dakota. Table 2 lists the Field of View (FOV) and noise statistics assumed for each station[10]. Three measurement scenarios are compared with range only, angles only, and the combination of range and range-rate. It is assumed that angle measurements are given as an azimuth and elevation pair. To ease implementation, the same noise parameters are used for each sensor, with range noise set at 30 meters and angle noise at 0.014°. Neither measurement type gives direct information about the velocity components. For accuracy comparison purposes, range rate was also included in this study, even though radar stations typically do not provide this measurement type. The range-rates are assumed to have noise at 5 cm/s levels.

Table 2: Radar station FOV limits and noise statistics

	Field of View			***Noise Statistics (from Vallado)***		
Site Location	**Range (km)**	**Azimuth (deg)**	**Elevation (deg)**	**Range (m)**	**Azimuth (deg)**	**Elevation (deg)**
Eglin FL	[100 , 3000]	[155 , 205]	[10 , 35]	32	0.0154	0.0147
Cavalier ND	[100 , 3000]	[313 , 63]	[10 , 50]	28	0.0125	0.0086
Shemya AK	[100 , 3000]	[289 , 349]	[10 , 50]	2.9	0.054	0.053

Figure 1 displays the radar station and FOV geometries. The deployer is in a polar orbit, and will cut across the U.S. from North to South on in the first orbit, being observed by Cavalier AFB first. The data throughout this report are presented during critical phases and color coded consistently. *Blue* shows the deployment phase occurring 75 seconds after injection. *Orange* is the first contact occurring 10 minutes after deployment and lasting for 2.5 minutes. *Yellow* is the second contact an orbit later (93 minutes), lasting only a few seconds. It is in the far left section of the

Cavalier FOV in Figure 1. Not all the targets are in the FOV simultaneously during this contact. The third contact (*purple*) occurs several orbits later (4.7 hours) from Shemya and lasts for one minute. Finally, the fourth (green) contact is from Eglin 4.2 hours later and lasts 3 minutes.

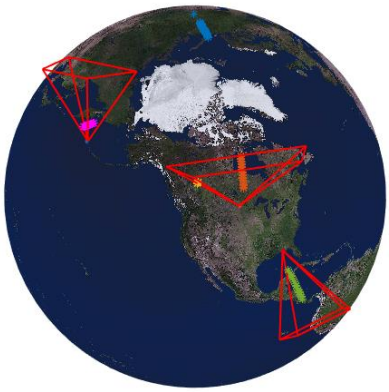

Figure 1: Location of radar stations and the respective sensor fields of view (FOV)

CPHD IMPLEMENTATION

For this study, a CPHD filter was implemented in MATLAB based on Vo [13] and incorporating the logarithmic form of the equations to insure numerical accuracy for the relative large number of targets (89) considered. Modifications were made to only perform measurement updates when one or more objects are within a sensor FOV. We also incorporated the approach proposed in [14] to allow the assigned probability of detection to be dependent on whether the target is expected to be within the sensor FOV.

Finally, for this initial study of acquisition and tracking of objects in the Cubesat cluster deployment scenario, we neglected the possibility of birthing, spawning, and clutter in the CPHD filter. The justification for this is approach is that all the ground-based observations are expected to be taken after all the Cubesats have been deployed, and the duration of the scenario is short enough that new objects are unlikely to appear during this time. Clutter was ignored to get an idea of the best possible performance that could be achieved. Once incorporated it can be expected to degrade the overall performance.

SCENARIO DISCUSSION

Several aspects make this a challenging and interesting scenario for study. Each Cubesat is deployed with a DV of only 1.5 m/s, with 2 seconds separating deployments within the same group. Such small perturbations do not produce sufficient separation distance to insure that the ground sensors can make distinct measurements 10 minutes later at the time of the first contact. Specifically, in our simulation, the minimum separation distance of any two Cubesats at the start of the first contact was found to be only 16 m, with a maximum separation of 2.1 km. These objects are assumed to be tracked from the ground with relatively coarse sensors. Range measurement noise is modeled as having a standard deviation of 30 m and angle measurement noise is assumed to be 0.014 deg. The latter maps to approximately 400 meters of error when the CubeSat's trajectory first enters the radar station FOV at low elevations. The 89 object simulation produces 78 pairs of Cubesats with separation distances within the ranging uncertainty of 30 meters, and 1,014 pairings with separation distances less than angle uncertainty of 400 meters.

Figure 2 shows the separation distances between each object at contact 1. The data plotted considers every target to every other target, hence the symmetry in the plot. Red lines are overlaid at

30 meters and 400 meters - the measurement noise floor due to range and angle measurements, respectively. The bands between 1.6 and 2.1 km show the separation between the two clusters; that is, those ejected in the deployer forward-velocity direction versus those in the anti-velocity direction. The single dotted line through the middle (around 1 km) is the deployer which is in between the two clusters. Along the bottom of the plot are the separation distances within a cluster, where the thick bands are an artifact of the 10 second delays between groups. Both clusters traverse the U.S. immediately after launch directly through the Cavalier FOV; however during this pass, the Cubesats are so closely spaced that they are very difficult to isolate with the ground sensor measurement accuracies assumed here.

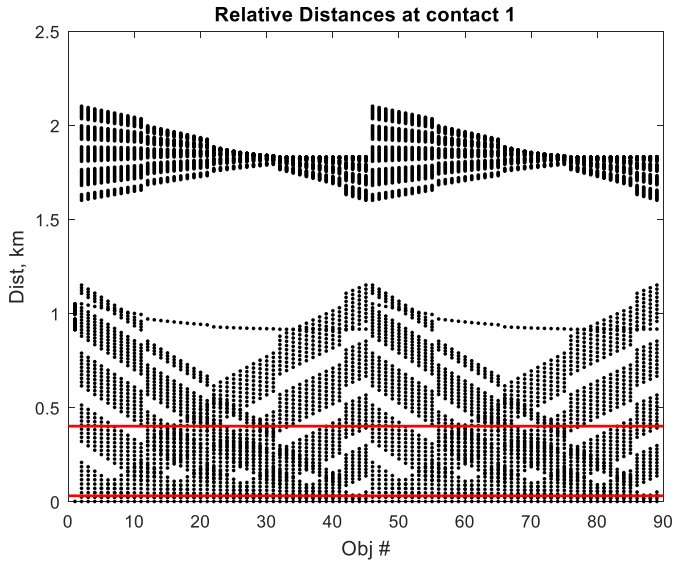

Figure 2: Relative distances at the start of Contact 1.

Another element of this scenario that makes estimation difficult is the sparse measurements. The second contact occurs only one orbit after deployment. While this might be expected to be ideal timing for observing the newly launched satellites; unfortunately, the cluster just skirts the FOV of the Cavalier station. Hence, at each time step, only a handful of the satellites are observed. This demands a variable probability of detection for objects tracked by the filter. This can have a detrimental effect on the cardinality calculations if the probability of survival is set too low. Even though all the objects may be observed during the second contact, the cardinality may drop because all the objects are not observed simultaneously.

The third contact is 4.7 hours later. By this time the Cubesats have spread out sufficiently above the noise floor for range measurements. The minimum separation is 34 meters with a maximum of 203 km between the two clusters. Figure 3 highlights the cluster separation in radial and in-track directions. There are still 52 pairings with separations less than 400 meters. At this point the measurements can be more effective, because the objects have sufficiently spread apart allowing better correlations. However, the separation benefit is tempered by growth in the state errors and uncertainties due to propagation in the absence of measurements. As a result, the filter can end up incorrectly predicting when objects will enter the sensor FOV.

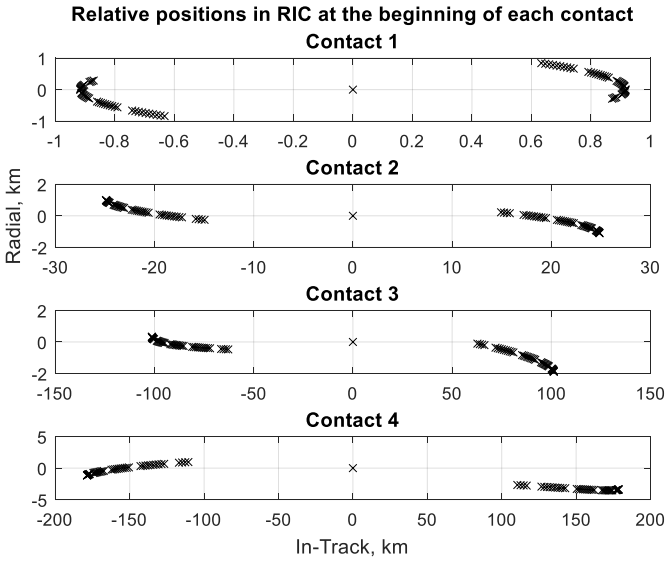

Figure 3: Cluster separation through the scenario. At the start of each contact all the objects are rotated to RIC relative to the deployer. Little cross-track variation is present.

FILTERING RESULTS

This section presents the results of filtering the three measurement scenarios. Table 3 provides the apriori uncertainties and filter tuning parameters used to generate the results.

Table 3: Apriori uncertainties and tuning parameter values used.

Scenario Parameter	Uncertainty
Apriori state position	5 m
Apriori state velocity	0.5 mm/s
DV error	1 %
Deployer rotation	1 %
Filter Parameter	**Value**
Probability of survival	0.9999
Probability of detection	0.985
Pruning threshold	1e-5
Merge distance	4
OSPA c value	1
OSPA p value	1

Since the CPHD does not explicitly estimate the state of specific objects, it can be a challenge to assess the orbit estimation accuracy. When tracking a single target with an extended Kalman filter an analyst typically compares the estimated error residuals with the 3 sigma uncertainty levels. However the CPHD filter updates the covariance of the constituent Gaussian components of the posterior intensity[11]. These are, strictly speaking, uncertainties of the PHD intensities and not state uncertainties. The uncertainties can only be loosely interpreted as state uncertainties.

The Optimal Sub Pattern Assignment (OSPA) metric is one tool used to assess the performance of a multi-target filter[12]. See Equation 1, where $\bar{d}_p^{(c)}$ is the OSPA metric of order p and cut-off c.

The term $d^{(c)}$ is the distance between the true and estimated objects positions cut-off at c. Calculating the OSPA requires setting these two tuning parameters c and p. The c value can be viewed as the point in which it is assumed that custody is lost. A value of 1 km was found to work well for this application. The p value is set to 1, to allow a direct interpretation of the metric. See Reference 12 for a discussion of the parameters.

$$\bar{d}_p^{(c)}(X,Y) \coloneqq \left(\frac{1}{n}\left(\min_{\pi\in\Pi_n}\sum_{i=1}^{m} d^{(c)}\left(x_i, y_{\pi(i)}\right)^p + c^p(n-m)\right)\right)^{\frac{1}{p}} \tag{1}$$

Figure 4 shows the OSPA values in the left plot for the three scenarios under study. The figure shows that the measurement types have similar performance through the second contact; however, after that there are significant performance differences between them. The discontinuities in the OSPA values occur because of time gaps between the contacts. At the end of the fourth contact, the OSPA values indicate that the angles-only scenario is the worst with respect to estimating the number of objects and their tracks while the range and range-rate scenario is the best. This intuitively makes sense as the range-rate observations provide direct information about the velocity components. Also the angles-only performs the worst because the angle noise from radar stations is very coarse at 0.014 degrees.

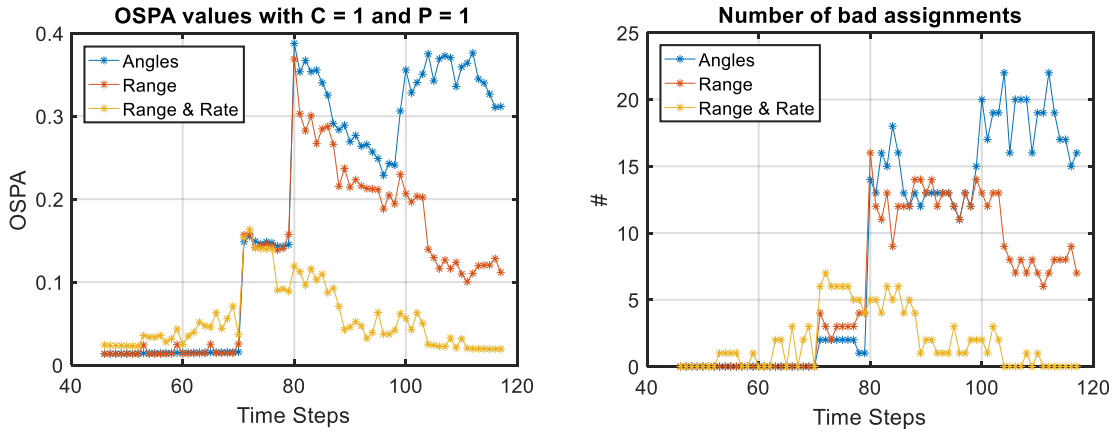

Figure 4: OSPA values for the three measurement scenarios on left. Number of bad assignments for each scenario on right. Data is collapsed in time, with time steps on the x-axis.

Despite its utility, the OSPA metric does not address all aspects of the tracking problem. Specifically it does not fully capture the accuracy of the state estimates with respect to their uncertainty or the correct distribution of discrete objects to particular clusters. Uncertainty is not incorporated at all in the OSPA calculation. Cardinality errors are included in the OSPA calculation; but there is no way with this metric to identify cardinality specific to a cluster. In our scenario there are two clear groups of objects, so a correct overall cardinality that does not reflect the number of objects in each group can be considered rather limited in its utility. The right plot of Figure 4 shows the number of incorrect object assignments resulting in errors from the true positions greater than the OSPA c value (1 km). Nonetheless, we rely on the OSPA metric because of the difficulty of capturing useful information for such a large number of objects individually.

To explore further the individual object results, Figure 5 shows the post-fit residual errors and 3 sigma uncertainties during each of the four contacts for the angles-only case. The data points in Figure 5 are color coded by contact and plotted against observation time step (rather than elapsed time). This suppresses the time gaps between the contacts that were described previously in the

Simulation Observables section. Since the CPHD does not have labels, estimated targets are associated with the true targets independently after each iteration of the filter updates. The assignments are taken from the Hungarian method[13] implemented in Vo's published code to calculate the OSPA distances $d^{(c)*}$.

Figure 5 does not include position errors for the bad assignments or mismatches shown in the right plot of Figure 4. The total number of omitted data points is given in the text box inserted in the upper plot of Figure 5. Mismatched or poor assignments occur because the filter has a tendency to output too many estimates in one of the clusters and too few in the other. Then when attempting to find unique assignments of estimated targets to each true object in the OSPA calculation, there will be some assignments across the gap between clusters. This would produce large outliers, on the scale of the cluster separation, which would swamp the intra-cluster positioning errors shown in Figure 5.

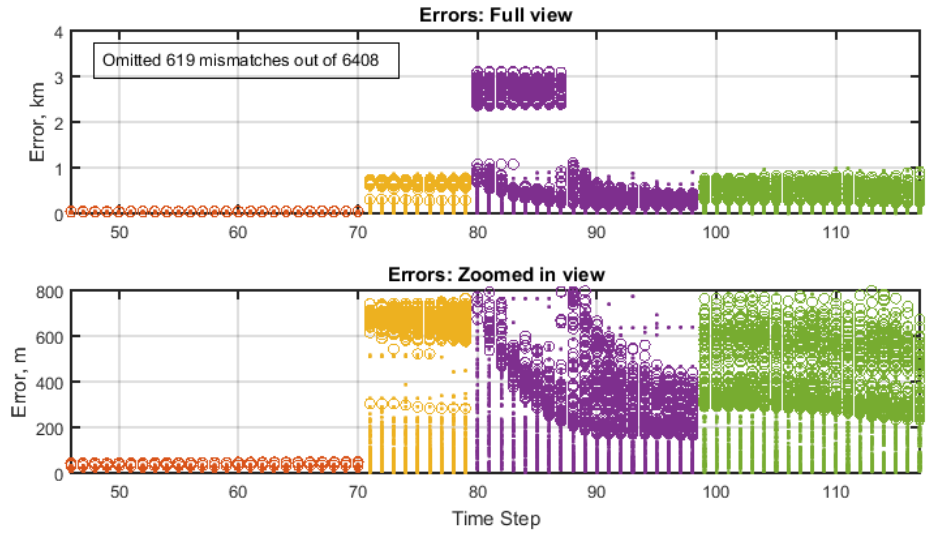

Figure 5: Post fit residual errors (dots) and 3 sigma uncertainties (circles) for a filter run with azimuth and elevation measurements only. Color coded by contact.

What is shown in Figure 5 provides some insights into the filter performance and scenario behavior; namely, when properly assigned within their cluster, most estimated targets are within the 3 sigma filter uncertainties. The expected growth in uncertainty between observation opportunities is present. Zooming in further to look at the residual errors (bottom plot of Figure 5) during the first contact shows that there is minimal refinement of the estimated states based on these measurements. This makes sense because the angle-only measurements have significant noise and the uncertainties map into large errors in the state space, often larger than the actual differences between states of the Cubesats within the cluster.

A deeper investigation of the errors at the beginning of the second contact shows larger error growth than was anticipated. The undesirable behavior was due to an inherent deficiency of the CPHD filter - that it lacks labels. In the merging step of the filter those components of the Gaussian mixture of estimated PHD locations that are close together (found through a Mahalanobis distance check) are combined as a weighted average based on the intensities. See the discussion on 'spooky action at a distance' for more details[14].

---

* Vo, B.T., Codes. Retrieved May 2, 2017, from http://ba-tuong.vo-au.com/codes.html

During the third contact (purple data between time step 80 and 98) the uncertainties collapse in two separate groups. This is because the cluster launched in the forward velocity direction passes through the radar FOV first, thus those estimates are updated first. Then the second cluster passes into the FOV around time step 88.

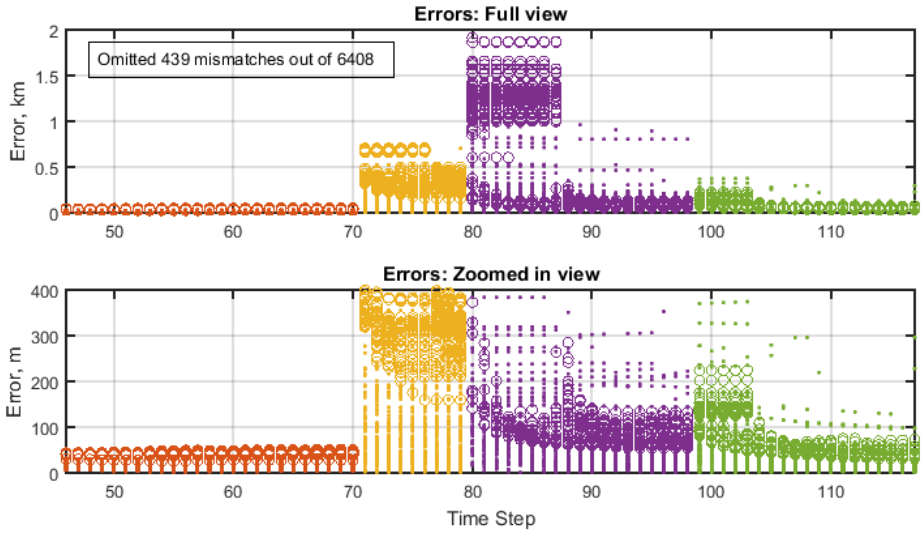

Figure 6: Post fit residual errors (dots) and 3 sigma uncertainties (circles) for a filter run with range measurements only. Color coded by contact.

For completeness, the range-only residual errors are provided in Figure 6. Generally, the results and interpretations are similar to those of the previous plots. Here the uncertainties collapse to smaller values, under 100 meters at the end versus 300 to 800 meters in the angles-only case. Again minimal updating occurs during the first contact. Fewer assignments are ignored in this plot, 439 versus 619 in Figure 5. With the less noisy range measurements, the CPHD filter is able to estimate more targets in the correct cluster.

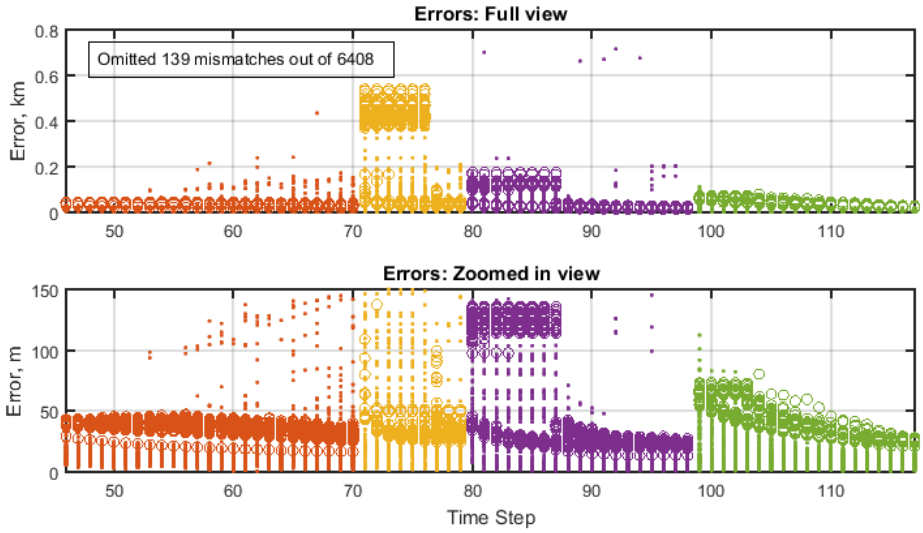

Figure 7: Post fit residual errors (dots) and 3 sigma uncertainties (circles) for a filter run with range and range-rate measurements. Color coded by contact.

Lastly the range and range-rate case is provided in Figure 7. Here the uncertainties are updated to very small values, under 50 meters by the end of the scenario. Only 139 bad assignments are omitted in the position error plot. Unlike the previous two cases where there was minimal improvement during the first contact, with range and range-rate measurements there is enough resolution to allow updates during the first contact as can be seen in the zoomed in lower subplot (orange section).

TUNING DISCUSSION

An important aspect of this work was understanding the tuning of the filter. Several lessons learned are discussed in the following.

The probability of survival specified in the CPHD significantly influences the cardinality prediction. Setting the value too low causes the cardinality to drop quickly, especially when observations are sparse. If all of the targets remain in the FOV this issue is avoided. But for a realistic clustered deployment this assumption doesn't always hold, as demonstrated by the second tracking interval in our simulation. Another concern that arises when contacts are spread out over several orbits, is that the survival probability is not specified as a function of time interval. The nominal prediction calculation does not take into account any difference between a 10 sec separation versus a 4.7 hour separation between measurements. It seems reasonable that the survivability should be influenced by either the time between updates or possibly based on the state uncertainty. That is, one might assign a lower probability of survival to a less certain target.

Probability of detection threshold also becomes an issue in sparse data sets. The CPHD implementation must include variable detection probabilities in sparse data sets. If measurements are sparse then every measurement is important. The simplest implementation is a binary switch based on whether the estimated target is in the FOV. It was noticed that there was better associations made when the detection probability was set to a lower value, however the cardinality would suffer by being over estimated if set too low. A detection probability of 98% represented a break point for our simulation. With a value too low the filter would output more estimates, which increased the chances that there would be at least 44 estimates output from each of the two clusters. This allowed there to be fewer bad assignments in the error plots. However, there were also estimates that were not associated with true objects. Additional rigorous study of the effects of varying the detection probability are warranted.

Estimated targets are identified through the intensities. The sum of the intensities should be equal to the cardinality. An interesting behavior of the intensities is that there is no mathematical requirement that they be binary. For example, there may be intensities closer to 2 implying that estimated state should be counted twice. Under some circumstances this will also make it impossible for the filter to output the number of unique targets that the cardinality indicates should be present. A strategy to mitigate this effect is to set the estimated cardinality to the minimum of either the predicted cardinality, or the number of unique intensities (estimated states) present.

Another phenomena of the filter is the 'spooky action at a distance' problem[14]. There are a lot of intensities in the Gaussian mixture implementation. A merging step is typically implemented which will decrease the number of intensities output by the filter. The merging step creates a weighted average estimated state to be output, thus creating the spooky action problem. One proposed idea to deal with the spooky action is to split the multi-target state into non-interacting populations, which could also aid in the identifying the correct number of estimates in both clusters[15].

The OSPA c value should be set somewhere between the separation distances between the targets and the maximum value that still allows one to claim custody of the target. In the Cubesat

cluster deployment scenario, the distance between two Cubesats may be as small as several meters, and as large as hundreds of kilometers. The results presented were generated with a c value of 1 km, which limits the maximum contribution of any one assignment to this level. In comparing results for different c values, we found that setting the c value lower results in a few nearly perfect assignments where they exist, while everything else is poorly assigned. Higher c values strike a balance with the bulk of the assignments being good, and only a few poor mismatches. Adjustment to the p value was not assessed in this work.

CONCLUSIONS

This work focused on the ability of a CPHD filter to estimate the state of objects present in a clustered environment based on a realistic Cubesat deployment scenario. In general, the CPHD filter is able to estimate the objects present in two separate clusters of Cubesats. With angle-only measurements the noise is so large that estimated states are hundreds of meters in error from the truth. Using range-only measurements the final errors are within tens of meters. Since the minimum true separation of objects at the end of the scenario is 40-50 meters, range measurements are necessary to provide the resolution to identify individual objects.

For both measurement types, the earliest possible contact observing the objects is not providing useful data because the objects are still too close together. To obtain useful observables there needs to be sufficient time for the natural effects of the dynamics to spread out the objects. The earliest contact at which respectable track estimates could be provided under this type of scenario is at least 10 hours later, at the end of the fourth contact. To provide quality tracking sooner would require changes to the deployment strategy. There would need to be longer spacing in time between deployments and/or larger velocity magnitudes imparted to the Cubesats. If range-rate or Doppler can be provided as an observable then measurements are more useful early on in the mission for object differentiation.

This scenario highlighted the complications that arise from tracking only from the ground with sparse, imprecise measurements. Situations where all the targets are not in the FOV simultaneously complicates the cardinality solution and exposes some aspects of the CPHD which may be undesirable for space object tracking. While the CPHD can handle this scenario, there are several issues hampering the effectiveness for clustered deployment of space objects. The lack of labels makes it difficult to assess the filter behavior with respect to track error. Also the lack of labels allows the 'spooky action' to introduce errors into the filter estimates early in the process. It is also assumed that labels would prevent the filter from outputting too few estimated targets in one of the clusters.

This paper discussed the effectiveness of the tools used to assess filter performance and the tuning of the filter's parameters. The OSPA metric is a convenient tool to judge the filter behavior, however it needs to have properly tuned input parameters appropriate for the specific scenario. In our simulation the OSPA values gave little indication that the filter was not properly estimating the correct number of objects in each cluster. A check of how many associations were larger than the cut-off c value did provide valuable insight into the scenario behavior. Unfortunately, the OSPA alone did not fully represent the accuracy of the estimated Cubesat states.

FUTURE WORK

The next step for our work will be to assess more recent filters developed that include track labels such as the GLMB filter[8]. This is expected to reduce the errors as well as avoid the spooky action at a distance issue. Future studies will also include more realistic and differentiated dynamics among the satellites. One of the topics of that will be interesting to study is the ability to detect maneuvers within labeled multi-target filters.

The initial states of the deployer were assumed to be given in lieu of performing initial orbit determination. This was done to concentrate on the filter performance with respect to the number of objects tracked, observation types, and cadence effects. Future work will include implementation of an initial orbit determination algorithm with the tracking algorithm.

ACKNOWLEDGMENTS

The authors would like to thank Dr. Brandon Jones for his numerous insights into the behavior of the CPHD filter. Much of this work was influenced by the efforts of Dr. Steve Gehly on his dissertation research.

REFERENCES

[1] Segerman, A. M., Byers, J. M., Emmert, J. T., & Nicholas, A. C. (2014). "Space Situational Awareness of Large Numbers of Payloads from a Single Deployment." *Advanced Maui Optical and Space Surveillance Technologies (AMOS).* Maui, HI.

[2] Gangestad, J. W., Rowen, D. W., Hardy, B. S., & Hinkley, D. A. (2014). "Flying in a Cloud of CubeSats: Lessons Learned from Early Orbit Operations of Aerocube-4, -5, and -6." *65th International Astronautical Congress.* Toronto, Canada.

[3] Ewart, R. M. (2016). "Enhanced Space Object Identification: Taking the Guesswork out of LEO CubeSats." *AIAA SPACE.* Longbeach, CA.

[4] Rivers, T. D., Heskett, J., & Villa, M. (2015). "RILDOS: A Beaconing Standard for Small Satellite Identification and Situational Awareness." *29th Annual AIAA/USU Conference on Small Satellites.*

[5] Rendleman, J. D. and Mountin, S. M., "Responsible SSA Cooperation To Mitigate On-orbit Space Debris Risks," *7th International Conference on Recent Advances in Space Technologies (RAST)*, IEEE, 2015.

[6] Weeden, B. (2015). "Overview of Space Debris and Cubesats." *NRC Committe on Cubesats for Science.* Washington, DC.

[7] Kennewell, J. A., & Vo, B.-N. (July 9-12, 2013). "An Overview of Space Situational Awareness." *16th International Conference on Information Fusion*. Istanbul, Turkey.

[8] Vo, B.-T., & Vo, B.-N. (2013). "Labeled Random Finite Sets and Multi-Object Conjugate Priors." *IEEE Transactions on Signal Processing, 61*(13), 3460-3475.

[9] Puig-Suari, J., Zohar, G., & Leveque, K. (2013). "Deployment of CubeSat Constellations Utilizing Current Launch Opportunities." *Small Satellite Conference.* SSC13-V-5.

[10] Vallado, D. A. (1997). Fundamentals of Astrodynamics and Applications. New York: McGraw-Hill. Table 4-4, pg 259.

[11] Vo, B.-N., & Ma, W.-K. (2006). "The Gaussian Mixture Probability Hypothesis Density Filter." *IEEE Transactions on Signal Processing*, 54(11), 4091-4104.

[12] Schumacher, D., Vo, B. T., & Vo, B. N. (2008). "A Consistent Metric for Performance Evaluation of Multi-Object Filters." *IEEE Transactions on Signal Processing*, 56(8), 3447-3457.

[13] C. H. Papadimitriou and K. Steiglitz, Combinatorial optimization; algorithms and complexity. Dover Publications, 1998.

[14] Franken, D., M. Schmidt, and M. Ulmke. "" Spooky action at a distance" in the cardinalized probability hypothesis density filter." *IEEE Transactions on Aerospace and Electronic Systems* 45.4 (2009).

[15] Jones, B.A., Hatten, N., Ravago, N., and Russell, R.P., (2016) "Ground-based Tracking of Geosynchronous Space Objects with a GM-CPHD Filter" *Advanced Maui Optical and Space Surveillance Technologies (AMOS).* Maui,HI.